Vietnam Journal of Marine Science and Technology; Vol. 21, No. 3; 2021: 259–270
DOI: https://doi.org/10.15625/1859-3097/16074
http://www.vjs.ac.vn/index.php/jmst

Suspended sediment floc size in the Cam - Nam Trieu estuary (Hai Phong, Vietnam), in wet season

Vu Duy Vinh[1,*], Sylvain Ouillon[2,3], Nguyen Minh Hai[1]

[1]*Institute of Marine Environment and Resources, VAST, Vietnam*
[2]*UMR LEGOS, University of Toulouse, IRD, CNES, CNRS, UPS, 14 avenue Edouard Belin, 31400 Toulouse, France*
[3]*Department Water-Environment-Oceanography, University of Science and Technology of Hanoi (USTH), VAST, Vietnam*
[*]E-mail: vinhvd@imer.vast.vn

Received: 18 May 2021; Accepted: 23 August 2021

Abstract
Median diameters (D_{50}) of suspended particles were inferred in the wet season in the Cam - Nam Trieu estuary (Hai Phong, Vietnam) based on the particle size distribution measured by LISST-100X on five transects along the river from 23 to 26 September 2015. The results showed that floc diameters varied between 3.6 µm to 146.5 µm and averaged 49.14 µm. At high tide, the average floc size D_{50} was lowest (42.66 ± 11.55 µm). It reached the highest value in the ebb tide (62.87 ± 23.34 µm) and then decreased to intermediate values in the flood tide (48.75 ± 15.72 µm). The coefficient of variation of the mean floc size D_{50} was lowest in the high tide (27.05%), highest in ebb tide (37.13%), then intermediate in the flood tide (32.12%).

Keywords: Suspended sediment floc size, Cam - Nam Trieu estuary, Hai Phong, D_{50}, particle size.

Citation: Vu Duy Vinh, Sylvain Ouillon, Nguyen Minh Hai, 2021. Suspended sediment floc size in the Cam - Nam Trieu estuary (Hai Phong, Vietnam), in wet season. *Vietnam Journal of Marine Science and Technology, 21*(3), 259–270.

INTRODUCTION

The particle size of suspended sediment is one of the important characteristics because it can reflect the sediment source and erosion [1–3], affect the entrainment, transport, and deposition processes [4, 5], and can be used to infer the contaminant sources [6, 7]. Sediment usually carries the signature of upstream disturbances in runoff and erosion to downstream channels [8]. Previous studies used particle size characteristics to trace suspended sediment in the river systems [9]. Walling and Moorehead (1989) [10] found that considerable variation existed in the particle size characteristics of sediment from different rivers in response to variations in source material and other physiographic controls. Jia et al., (2016) [11] also demonstrated that particle size characteristics were useful in determining sediment provenance in the Yellow river basin based on the sediment deposits in the river system, which mainly comprised coarse sand particles larger than 0.05 mm.

Further, the grain size of suspended sediment and its variation in river flows is essential information for modeling river sediment transport, reservoir siltation and sediment particles' in various environmental processes [4, 12, 13]. The transport of sediments, both in suspended and bedload form, is critical for controlling coastal morphology. The size of the transported particles can be a factor in distinguishing between suspended load and bedload [14]. For example, smaller (i.e., < 0.05 mm) and lighter particles (including organic material) are typically transported in suspension in flowing water. Heavier particles (i.e., in the range of 0.1–100 mm) can be transported as bedload, rolling, or bouncing along the channel bed.

The grain size of suspended sediment also is an important parameter to estimate setting velocities of the sediment particles [15, 16] and is essential for various theoretical analyses and engineering applications, such as sediment transport, suspension [17, 18], deposition, mixing and exchange processes [16].

The previous studies showed that in estuaries and coastal waters, the most significant particles are those of lithogenic (inorganic) and detrital (organic) particles with sizes in the range from clay to gravel (0.0039–200 mm) according to the classification on the Udden-Wentworth scale [19, 20]. In coastal hydraulic theory, the grain size analysis is performed for either individual particles or their hydraulic equivalents. The median diameter denoted D_{50}, corresponding to 50% of finer and 50% of coarser particles and inferred from the cumulative volume of suspended aggregates, is widely utilized to describe the sediment size distribution curve without considering the shape of sediment grains.

The Cam - Nam Trieu estuary (figure 1a) is located in Hai Phong city (Northeast Vietnam). This area, also known as an extensive ports system, is the main gate to connect North Vietnam to the world market. Harbors in Hai Phong city are in the Cam - Nam Trieu estuary and create the second-largest port system in Vietnam. However, Hai Phong harbor has been affected by increasing siltation. The sediment volume dredged to maintain a minimum depth of the navigation channels was about 0.78×10^6 m^3 in 2013 and 1.17×10^6 m^3 in 2015 [21]. Many studies were recently devoted to find the cause of siltation in the navigation channel deposition and to propose solutions, focusing on geomorphology [22], geology [23], hydrodynamics, and sediment transport [24–26]. Recently, Vinh et al., (2018) reported the estuarine turbidity maxima's characteristic parameters and investigated their tidal variations within the Cam - Nam Trieu estuary (North Vietnam) during the early wet season. This study also presented the link between Estuarine Turbidity Maxima (ETM) and settling velocity characteristics during the early wet season [27]. However, these parameters were susceptible to environmental conditions that changed very much in this region. Therefore, this study examined suspended sediment particle size distribution in the wet season in Cam - Nam Trieu estuary. These results will be the basis for research on sediment dynamics in the study area.

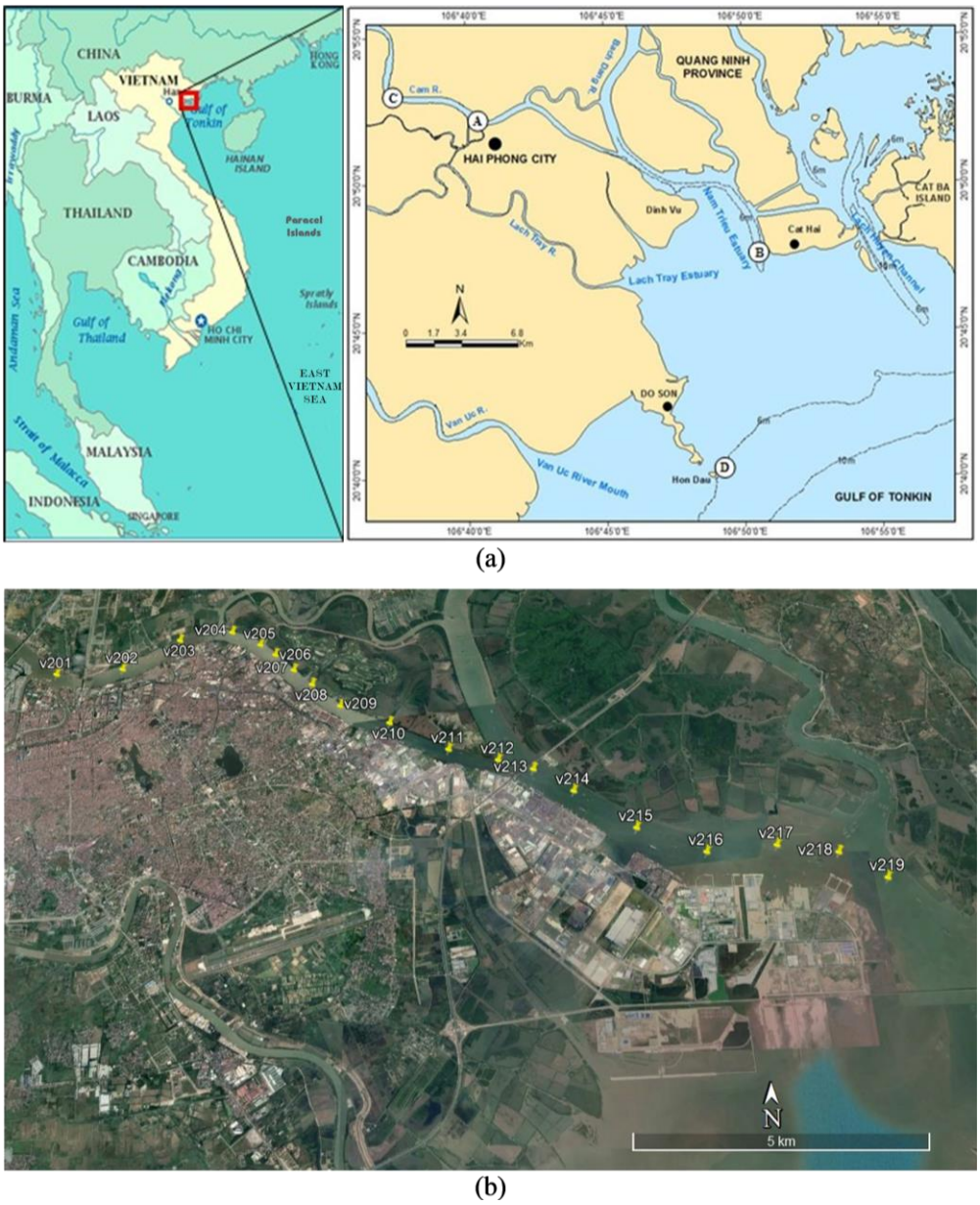

Figure 1. The Cam - Nam Trieu estuary (a) general location-transects were mostly performed between stations A and B, C is the hydrological station, D is the tide gauge at Hon Dau; (b) example of survey (stations of Transect 4) along the A-B transect (from Vinh et al., (2018))

MATERIAL AND METHODS

The Cam - Nam Trieu estuary

The present study is based on measurements performed along the Cam river estuary and in the Nam Trieu estuary; this area is referred to as the Cam - Nam Trieu estuary. The Cam - Nam Trieu estuary is located in Hai Phong (the third-largest city of Vietnam), northeastern Vietnam (figure 1.1a). This estuary receives water and sediment from the Cam river and the Bach Dang river. Although the Cam and Bach Dang rivers belong to the Thai Binh river, they also receive water and sediment from the Red river through the Duong river (see a map of connections within the Red River delta in Vinh et al., [24]). The total river

discharge through the Nam Trieu estuary to the coastal zone is about 20×10^9 m^3 $year^{-1}$, corresponding to 16.5% of the total water discharge from the Red - Thai Binh river system to the Tonkin Gulf [24].

Annually, sediment flux from the Red - Thai Binh river through the Cam and Bach Dang rivers to the coastal zones was about 13.2×10^6 t, until the Hoa Binh dam impoundment in the 1980s. From this period, a large amount of riverine sediment has been trapped in the reservoirs. The sediment flux through the Cam and Bach Dang rivers to the coastal zones decreased to 6.0×10^6 t $year^{-1}$, in proportion to 17% of the total sediment of the Red - Thai Binh river to the Red river coastal area [24].

This area is influenced by a tropical monsoon climate with dry winter and wet summer. Based on measurements at Hon Dau from 1978 to 2007, annual rainfall in the region was 1,161 mm, which concentrated mainly in the summer (May to October), with 83% total of the year. The wind direction was dominantly (72.2%) from the East (NE, E, SE) and South (SW, S, SE) directions in the wet season (June to September), and from the North (NE, N, NW) and East (SE, E, NE) directions (92.1%) in the dry season (December to March), from wind data measured at Hon Dau (1960–2011).

Located in the Red river system, the Cam and Bach Dang rivers are strongly affected by their hydrological regime [25–29]. Based on data from 1960 to 2010, the Red river discharge at Son Tay (near the apex of the Red River delta) varied over the range 80.5 (2010)–160.7 (1971) $\times 10^9$ m^3 $year^{-1}$, with an average value of 110.0×10^9 m^3 $year^{-1}$. Water river discharge encompasses strong seasonal variations, with 71–79% of annual total water discharge in the rainy season and only 9.4–18% during the dry season [30]. The Cam - Nam Trieu estuary is affected by tides that are mainly diurnal [31]. Based on the tide gauge measurements at Hon Dau station (1960–2011), the tidal range is about 2.6–3.6 m in spring tide and about 0.5–1.0 m in the neap tide.

Field data

A field survey was performed in the Cam - Nam Trieu estuary during spring tide on 23–26 September May 2015. Five along river transects from the upper estuary in the Cam river (position A, figure 1a) to the Nam Trieu mouth (position B, figure 1a) or the reverse was performed with a total of 115 stations (see one of the six transects on figure 1b). At each station, depth profiles of floc size distribution and concentration were measured using an in situ laser scattering and transmissometers instrument with a 90% path reduction module (LISST-100X, Sequoia Scientific Inc. (Bellevue, WA, USA); e.g., [32–36]). The LISST of type B provided the volumetric particulate concentration in 32 logarithmically spaced size classes ranging from 1.25 μm to 250 μm and light attenuation at $\lambda = 660$ nm.

Data processing

The distribution of volume concentration of particles given by LISST-100X is discretized over the continuous spectrum of 32 size classes. Their sum is providing the suspended particle matter volume concentration. Particles less than the smallest size class or bigger than the largest size class affect the measurements in the spectrum. In this study, we followed the recommendation of literature to remove the first and last classes for calculating the general slope of the particle size distribution and the mean apparent diameter D_{50} [37–41]. Based on data between class #2 and class #31, D_{50} was calculated as the diameter corresponding to 50% of the cumulative volume concentration of aggregates between 1.48 μm and 212 μm.

The number of particles of each class, $N(D)$, was calculated from the volumetric particle size distribution (PSD), assuming spherical particles in the assemblage after normalization by the width of each logarithmically spaced size bin. The more often, a power-law relationship can be proposed between N and D following:

$$N(D) = aD^{-j} \quad (1)$$

Where: a is a coefficient (in a number of particles $L^{-1}\mu m^{-1}$); D is the diameter of aggregates; and j is the dimensionless exponent, also referred to as the particle size distribution slope or the Junge parameter [42, 43]. j provides information on the relative

concentration of slight to large particles: The steeper the slope, the more significant proportion of smaller particles, and the flatter the slope, the more excellent ratio of larger particles. Furthermore, *j* can be estimated from multispectral satellite data of ocean color through the particulate beam attenuation [44] or the particulate backscattering coefficient [45, 46]. For natural waters, *j* slopes generally vary from 3 to 5 with most values between 3.5 and 4 [47] and can be up to 7 for submicron particles in the ocean [46].

Due to the skip of the first class (< 1.48 μm) and the last class (> 212 μm) of the particle sizes, the remaining grain size range was analyzed through some groups: Over the whole particle size range (1.48–212 μm), the fine particle size group (1.48–17.7 μm), the medium particle size group (17.7–92.6 μm), and the coarse particle size group (92.6–212 μm). The classes were defined from our measurements to separate the two extreme peaks (around 3.4 μm and 120–140 μm) from the intermediate peaks about 25 μm or 45 μm. Other groups may have been considered (e.g., [48]). The purpose of the groups here is to illustrate the transfer of particles amongst them during the tidal cycle inferred by flocculation/disaggregation and/or sedimentation/erosion. The Junge parameter and aggregate settling velocity were also calculated for each of these three groups.

RESULTS AND DISCUSSION

Particle size distribution at high tide (transects 1 and 5)

The first transect was performed between stations v201 and v219 at high tide (water elevation = 1.3–2.5 m), 23 September 2015. The longitudinal profile of D_{50} distributions showed an increasing D_{50} value from 30 μm and 65 μm from the river to the estuary. Larger particle sizes (D_{50} > 50 μm) were observed near the bottom in the lower estuary (v213-v219). The biggest flocs were found at v213 and v215, with 60–65 μm. According to depth, D_{50} was almost smaller than 50 μm at the surface layer (0–4 m depth) and tended to increase at the bed layer (figure 2).

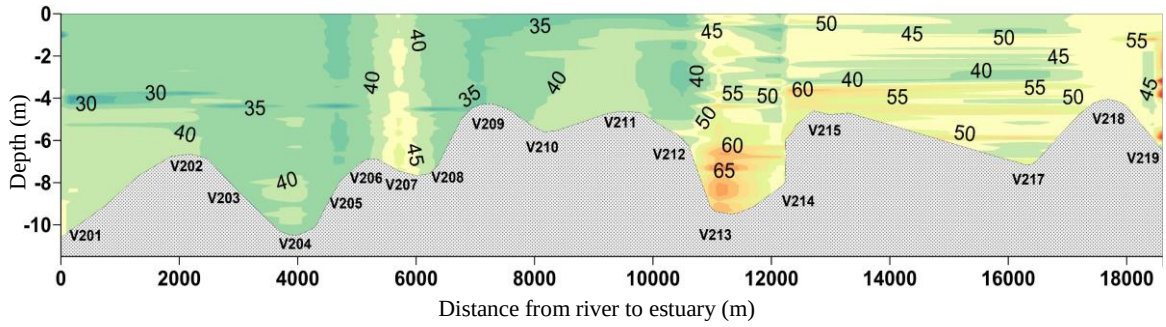

Figure 2. 2D distributions of D_{50} (μm) along transect 1, high tide (23 Sep., 2015)

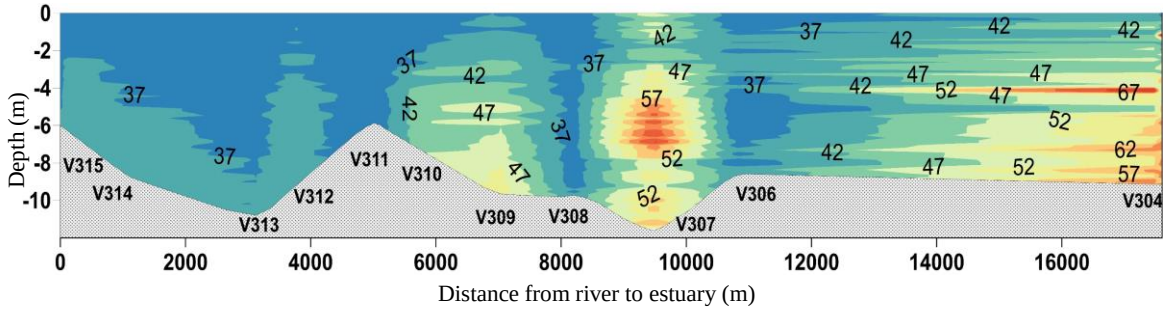

Figure 3. 2D distributions of D_{50} (μm) along transect 5, high tide (25 Sep., 2015)

Figure 3 shows the distribution of particle sizes (D_{50}) along transect 5 (v315-v304). The size of flocs varied from 37 μm to 67 μm. The bigger particle size was observed at the middle transect (v307) and the river mouth (v304), with a value of about 52–67 μm. Especially at the core area (4 m depth), flocs can reach 57 μm and 67 μm at the middle site and the mouth, respectively (figure 3).

Particle size distribution at ebb tide (transect 2)

The D_{50} values were measured during the ebb tide (water elevation below 0.7 m) on 23 September 2015 at transect 2 (v234-v220). The D_{50} values varied between 35 μm and 80 μm. They reached the highest values upstream (v234-v233) and near the mouth (v221), with 75-80 μm. The smallest particles were observed at a 3 km distance from A site (v229) and v220 (35–45 μm), especially at 2m depth of v220; the value only was 35 μm. Due to high stratification during the ebb tide, the distribution of D_{50} particles was different than at high tide. According to depth, different particle sizes are scattered (figure 4).

Particle size distribution at flood tide (transects 3 and 4)

D_{50} values were also measured along transect 3 (v236-v251) and transect 4 (v273-v300) during the flood tide. The results showed that the median particle sizes (D_{50}) varied between 40 μm and 85 μm. The highest values are near the mouth (v247 and v250), along the transect 4 at 65–88 μm, the lowest values were observed upstream to the middle region (almost smaller than 45 μm)). At transect 4, the largest particle sizes were found at the mouth (v295-v297) and upstream (v273-v274), with 65–85 μm. At the core area, they had the smallest, at 40–45 μm. According to depth, D_{50} tended to increase from surface to bottom (figure 5).

Particle size distribution in tidal stages

The mean variation of the suspended sediment floc size with tidal stages is analyzed (table 1). The results showed a significant difference in the mean values of D_{50} in the longitudinal transect during various tidal phases. Floc size D_{50} was smaller at high tide with a mean value of 42.66 μm and a low standard deviation (11.55 μm). In this time, while the minimum flocs size was only about 3.6 μm, the maximum value can reach 140.79 μm (table 1).

During flood tides, the maximum size of the flocs D_{50} along river transects was 142.48 μm, which was 118.46 μm, much higher than its minimum value. The mean floc size in this stage was bigger than in high tide, at 48.75 μm. The values of flocs size were spread out over a wider range; the standard deviation was about 15.72 μm (table 1).

The mean floc size of D_{50} in the ebb tide was the highest amongst the tidal stages, with 62.87 μm. Minimum and maximum floc sizes were 19.61 μm and 146.53 μm, respectively. The standard deviation was about 23.34 μm (table 1).

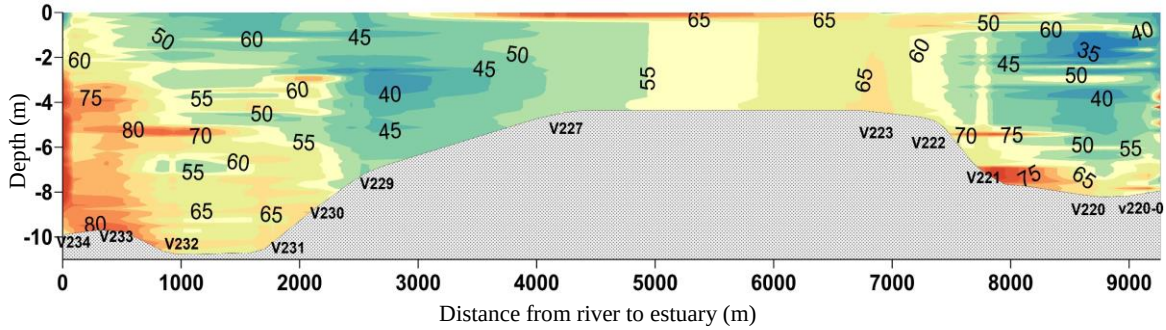

Figure 4. 2D distributions of D_{50} (μm) along transect 2, ebb tide (23 Sep., 2015)

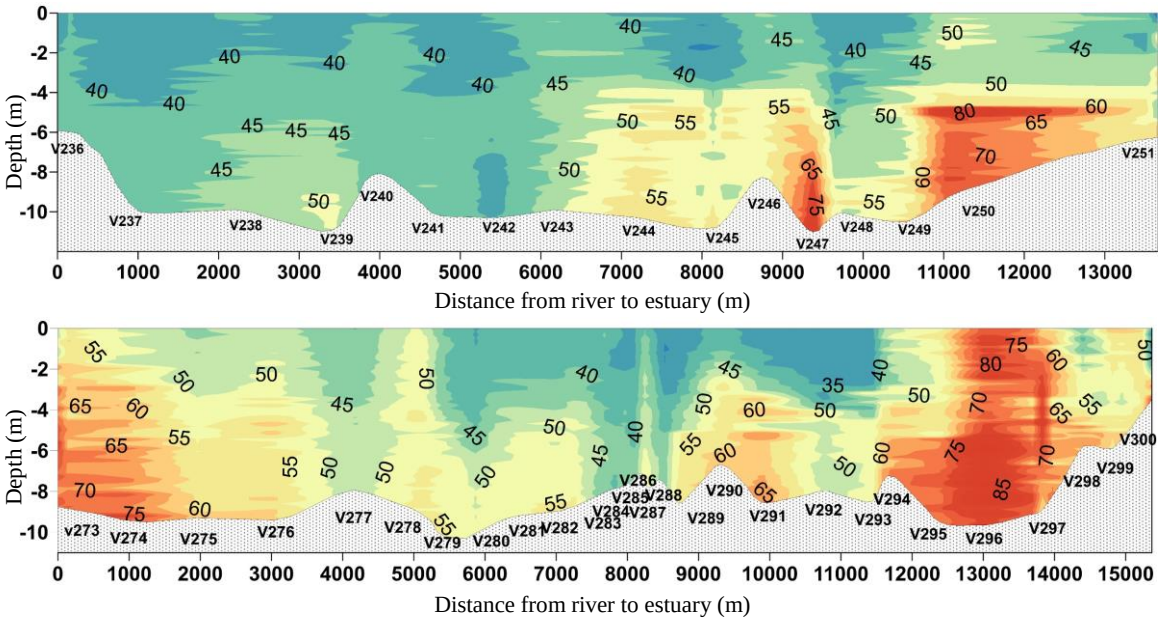

Figure 5. 2D distributions of D_{50} (μm) along transect 3 (24 Sep., 2015), above, and transect 4 (24 Sep., 2015), below, at flood tide

Table 1. Mean value of D_{50} (μm) in the longitudinal transects in September 2015

Tidal stage	Min.	Max.	Average	Standard deviation (SD)	Coefficient of variation CV(%)
High tide/transect 1	3.64	140.79	43.59	12.43	28.53
Ebb tide/transect 2	19.61	146.53	62.87	23.34	37.13
Flood tide/transect 3	30.60	142.48	46.50	13.79	29.65
Flood tide/transect 4	24.02	113.96	51.00	17.64	34.58
High tide/transect 5	31.20	88.80	41.73	10.67	25.57
Averagevalue at high tide	*17.42*	*114.80*	*42.66*	*11.55*	*27.05*
Average value in flood tide	*27.31*	*128.22*	*48.75*	*15.72*	*32.12*

DISCUSSION

The floc size can vary from a few micrometers to hundreds, even thousands of micrometers [49–52]. The variations in floc size are primarily due to flocculation processes, such as aggregation and breakup. In this study, suspended sediment floc size was calculated from *in situ* data at 115 stations from 5 transects in the wet season. The D_{50} values changed from 3.64 μm to 146.5 μm, and the range of average values was 41.73–62.87 μm. These results are in qualitative agreement with the previous study [26], which reported that the mean floc size at Cam and Dinh Vu estuary is in order 60 μm and 67 μm. In Yangtze Estuary, Guo et al., (2017) [53] reported a D_{50} range of 14–95 μm in the wet season. Wolanski et al. (1996) [54] showed that median particle sizes in the Mekong estuary varied between 50 μm and 80 μm in the flood season.

In this study, floc size of suspended sediment D_{50} in the Cam - Nam Trieu estuary is lower in the high tide (averaged 42.66 ± 11.55 μm), increased to 48.75 ± 15.72 μm at flood tide, and showed higher values in the ebb tide (62.87 ± 23.34 μm). The results also show that the coefficient of variation of the average floc size is lower in high tide (27.05%), increasing in flood tide (27.05%), and higher in ebb tide (37.13%). This trend is different from the previous study [27] in the early wet season. The median diameter of flocs was the lowest at

ebb tide (average D_{50} = 37.9 μm) and high tide (average D_{50} = 39.9 μm), intermediate at flood tide (averaged D_{50} = 45.9 μm). It was the highest at low tide (averaged D_{50} = 56.0 μm), showing a complicated variation of suspended sediment floc size with tidal stages. Wolanski et al., (1996) [54], based on the measurement data during 15–20 November 1993, reported that the relationship between tides and floc size was not clear, but the flocs were larger in freshwater. Another study also confirmed this at three stations in Cam, Bach Dang and Dinh Vu [26]. Their result reported that in the wet season: at the Cam station (in Cam river), floc size was larger at flood tide than at ebb tide; by contrast, at Bach Dang station, large floc size at ebb tide was more significant than at flood.

Meanwhile, at Dinh Vu station (in the lower part of Cam - Nam Trieu), floc size was dominant in the upper layer and larger near the bed during the flood tide. During the ebb tide, the distribution of moderate floc size values was more homogeneous in the water column, with values decreasing at the mid-ebb tide. Guo et al., (2017) [56] presented that the mean floc size was 43 ± 10 μm at neap tide in the wet season, about 57% larger than the spring tide in Yangtze estuary. Flocs were larger at high tide than low tide (the largest flocs occurred around high tide). Smaller flocs persisted at around peak flood and ebb tides.

Eisma and Li (1993) [55] also measured floc sizes in the Dollard estuary at three fixed stations. They also found that floc size reached a maximum during each ebb and flood tides and decreased again towards the slack tide. During ebb tide, the maximum floc size occurred during the maximum suspended-matter concentration or shortly after. During flood tide, the floc size continued to increase after the concentration maximum was reached. Maybe the increasing floc sizes towards high tide, as observed by Eisma and Li (1993) [55], were caused by horizontal advection of flocs from upstream areas. In these areas, towards the estuary's mouth, the current velocities are prominent and could have resuspended more large flocs. As we know, floc size results from a dynamic equilibrium between flocculation and breakup processes, and biological factors could mediate both processes.

On the other hand, the organic material can adhere to primary particles, change their surface charge, and increase the probability of cohesion after collision [56]. In the Cam - Nam Trieu estuary, Mari et al., [36] and Vinh et al., (2018) [27] also reported the role of salinity and co-varying factors on the aggregation/sedimentation processes, which has an important impact on the floc size of suspended sediment. Much related research on the tidal variation of flocs size did not show clear trends reported in previous studies [52, 54, 55]. Therefore, the results in this study are an additional contribution to an understanding of flocculation processes in tidal cycles.

CONCLUSION

This study examined the size of the in-situ flocs suspended sediment along the river transect of Cam - Nam Trieu estuary, based on measured data in the wet season 2015. Floc diameter was estimated from a LISST-100X. Floc diameters varied between 3.6 μm and 146.5 μm and averaged 49.14 μm. There is a horizontal variation of floc size within along Cam - Nam Trieu estuarine river transects. Areas with large floc sizes on the cross-section vary according to the tidal stages and water river discharges.

During the survey, the average floc size of suspended sediment in Cam - Nam Trieu estuary is lower in the high tide (averaged 42.66 ± 11.55 μm), increasing to 48.75 ± 15.72 μm in flood tide, with a higher value in the ebb tide (62.87 ± 23.34 μm). The results also show that the coefficient of variation of the average floc size is lower in high tide (27.05%), increasing in flood tide (32.12%), and higher in ebb tide (37.13%).

Acknowledgments: This work was financed by the science and technological cooperation program between the Vietnam Academy of Sciences and Technology (VAST) and the French "Institut de Recherche pour le Développement (IRD)" project QTFR01.01/20–21 and NĐT.97.BE/20. This paper contributed to the LOTUS International

Joint Laboratory (lotus.usth.edu.vn) and benefited from the support of the VAST05.05/21–22 project.

REFERENCES

[1] Xu, J., 2002. Implication of relationships among suspended sediment size, water discharge and suspended sediment concentration: the Yellow River basin, China. *Catena*, *49*(4), 289–307. doi: 10.1016/S0341-8162(02)00064-4

[2] Woodward, J. C., and Walling, D. E., 2007. Composite suspended sediment particles in river systems: their incidence, dynamics and physical characteristics. *Hydrological Processes: An International Journal*, *21*(26), 3601–3614. http://dx.doi.org/10.1002/hyp.6586

[3] Wendling, V., Legout, C., Gratiot, N., Michallet, H., and Grangeon, T., 2016. Dynamics of soil aggregate size in turbulent flow: Respective effect of soil type and suspended concentration. *Catena*, *141*, 66–72. https://doi.org/ 10.1016/j.catena.2016.02.015

[4] Walling, D. E., Owens, P. N., Waterfall, B. D., Leeks, G. J., and Wass, P. D., 2000. The particle size characteristics of fluvial suspended sediment in the Humber and Tweed catchments, UK. *Science of the Total Environment*, *251*, 205–222. doi: 10.1016/s0048-9697(00)00384-3

[5] Haritashya, U. K., Kumar, A., and Singh, P., 2010. Particle size characteristics of suspended sediment transported in meltwater from the Gangotri Glacier, central Himalaya—An indicator of subglacial sediment evacuation. *Geomorphology*, *122*(1–2), 140–152. doi: 10.1016/j.geomorph.2010.06.006

[6] Slattery, M. C., and Burt, T. P., 1997. Particle size characteristics of suspended sediment in hillslope runoff and stream flow. *Earth Surface Processes and Landforms: The Journal of the British Geomorphological Group*, *22*(8), 705–719. https://doi.org/10.1002/(SICI)1096-9837(199708)22:8%3C705::AID-ESP739%3E3.0.CO;2-6

[7] Smith, T. B., and Owens, P. N., 2014. Flume-and field-based evaluation of a time-integrated suspended sediment sampler for the analysis of sediment properties. *Earth Surface Processes and Landforms*, *39*(9), 1197–1207. https://doi.org/10.1002/esp.3528

[8] Sutherland, D. G., Ball, M. H., Hilton, S. J., and Lisle, T. E., 2002. Evolution of a landslide-induced sediment wave in the Navarro River, California. *Geological Society of America Bulletin*, *114*(8), 1036–1048. https://doi.org/10.1130/0016-7606%282002%29114%3C1036%3AEOALIS%3E2.0.CO%3B2

[9] Walling, D. E., and Woodward, J. C., 1995. Tracing sources of suspended sediment in river basins: a case study of the River Culm, Devon, UK. *Marine and Freshwater Research*, *46*(1), 327–336. https://doi.org/10.1071/MF9950327

[10] Walling, D. E., and Moorehead, P. W., 1989. The particle size characteristics of fluvial suspended sediment: an overview. *Sediment/Water Interactions*, 125–149. https://doi.org/10.1007/978-94-009-2376-8_12

[11] Jia, X., Li, Y., and Wang, H., 2016. Bed sediment particle size characteristics and its sources implication in the desert reach of the Yellow River. *Environmental Earth Sciences*, *75*(11), 1–13. https://doi.org/ 10.1007/s12665-016-5760-9

[12] Green, D. B., Logan, T. J., and Smeck, N. E., 1978. Phosphate adsorption-desorption characteristics of suspended sediments in the Maumee River Basin of Ohio. *Journal of Environmental Quality*, *7*(2), 208–212. https://doi.org/10.2134/jeq1978.00472425000700020011x

[13] Banasik, K., and Mitchell, J. K., 2008. Conceptual model of sedimentgraph from flood events in a small agricultural watershed. *Annals of Warsaw University of Life Sciences-SGGW. Land Reclamation*, *39*, 49–57. http://dx.doi.org/ 10.2478/v10060-008-0004-7

[14] Fan, J., and Morris, G. L., 1998. Reservoir Sedimentation Handbook: Design and Management of Dams, Reservoirs, and

Watersheds for Sustainable Use. *McGraw-Hill*.

[15] Guo, J., 2002. Logarithmic matching and its applications in computational hydraulics and sediment transport. *Journal of Hydraulic research*, *40*(5), 555–565. https://doi.org/10.1080/00221680209499900

[16] Zhiyao, S., Tingting, W., Fumin, X., and Ruijie, L., 2008. A simple formula for predicting settling velocity of sediment particles. *Water Science and Engineering*, *1*(1), 37–43. https://doi.org/10.1016/S1674-2370(15)30017-X

[17] Dietrich, W. E., 1982. Settling velocity of natural particles. *Water resources research*, *18*(6), 1615–1626. doi: 10.1029/WR018i006p01615

[18] Zhang, S., Jia, Y., Wen, M., Wang, Z., Zhang, Y., Zhu, C., ... and Liu, X., 2017. Vertical migration of fine-grained sediments from interior to surface of seabed driven by seepage flows–'sub-bottom sediment pump action'. *Journal of Ocean University of China*, *16*(1), 15–24. doi: 10.1007%2Fs11802-017-3042-0

[19] Udden, J. A., 1914. Mechanical composition of clastic sediments. *Bulletin of the Geological Society of America*, *25*(1), 655–744. https://doi.org/10.1130/GSAB-25-655

[20] Wentworth, C. K., 1922. A scale of grade and class terms for clastic sediments. *The journal of geology*, *30*(5), 377–392.

[21] Vietnam Maritime Administration (Vinamarine), 2017. Approved planning for dredging in Hai Phong port. Available online: http://www.vinamarine.gov.vn; accessed July 29 2017.

[22] Vuong, B. V., Liu, Z. F., Thanh, T. D., and Khang, N. D., 2013. Initial results of study in sedimentation rate and geochronology of modern sediments in the Bach Dang estuary by the methods of ^{210}Pb and ^{137}Cs radio tracer. In *Proceedings of the Second National Scientific Conference on Marine Geology, Ha Noi-Ha Long, Vietnam* (pp. 10–11).

[23] Thanh, T. D., Can, N., Nga, D. D., and Huy, D. V., 2004. Coastal development and sea level change during Holocene in Haiphong area. *Vietnam Journal Marine Science Technology*, *3*, 25–42.

[24] Vinh, V. D., and Thanh, T. D., 2012. Aplication numerical model to study on maximum turbidity zones in Bach Dang estuary. *Vietnam Journal of Marine Science and Technology*, *12*(3), 1–11.

[25] Vinh, V. D., and Van Uu, D., 2013. The influence of wind and oceanographic factors on characteristics of suspended sediment transport in Bach Dang estuary. *Vietnam Journal of Marine Science and Technology*, *13*(3), 216–226.

[26] Lefebvre, J. P., Ouillon, S., Vinh, V. D., Arfi, R., Panché, J. Y., Mari, X., Thuoc, C. V., and Torréton, J. P., 2012. Seasonal variability of cohesive sediment aggregation in the Bach Dang–Cam Estuary, Haiphong (Vietnam). *Geo-Marine Letters*, *32*(2), 103–121. doi: 10.1007/s00367-011-0273-8

[27] Duy Vinh, V., Ouillon, S., and Van Uu, D., 2018. Estuarine Turbidity Maxima and variations of aggregate parameters in the Cam-Nam Trieu estuary, North Vietnam, in early wet season. *Water*, *10*(1), 68. http://dx.doi.org/10.3390/w10010068

[28] Vinh, V. D., and Thanh, T. D., 2014. Characteristics of current variation in the coastal area of red river delta-results of resaerch using the 3D numerical model. *Vietnam Journal of Marine Science and Technology*, *14*(2), 139–148.

[29] Vinh, V. D., Baetens, K., Luyten, P., Tu, T. A., and Anh, N. T. K., 2013. The influence of surface wind on the salinity distribution and circulation in the coastal waters of the Red River Delta, Vietnam. *Vietnam Journal of Marine Science and Technology*, *13*(1), 12–20.

[30] Vinh, V. D., Ouillon, S., Thanh, T. D., and Chu, L. V., 2014. Impact of the Hoa Binh dam (Vietnam) on water and sediment budgets in the Red River basin and delta. *Hydrology and Earth System Sciences*, *18*(10), 3987–4005. doi: 10.5194/hess-18-3987-2014

[31] Minh, N. N., Patrick, M., Florent, L., Sylvain, O., Gildas, C., Damien, A., &

Van Uu, D. (2014). Tidal characteristics of the gulf of Tonkin. *Continental Shelf Research*, *91*, 37–56. https://doi.org/10.1016/j.csr.2014.08.003

[32] Traykovski, P., Latter, R. J., and Irish, J. D., 1999. A laboratory evaluation of the laser in situ scattering and transmissometery instrument using natural sediments. *Marine Geology*, *159*(1–4), 355–367. https://doi.org/10.1016/S0025-3227(98)00196-0

[33] Agrawal, Y. C., and Pottsmith, H. C., 2000. Instruments for particle size and settling velocity observations in sediment transport. *Marine Geology*, *168*(1–4), 89–114. http://dx.doi.org/10.1016/S0025-3227(00)00044-X

[34] Mikkelsen, O. A., and Pejrup, M., 2000. In situ particle size spectra and density of particle aggregates in a dredging plume. *Marine geology*, *170*(3–4), 443–459. http://dx.doi.org/10.1016/S0025-3227(00)00105-5

[35] Voulgaris, G., and Meyers, S. T., 2004. Temporal variability of hydrodynamics, sediment concentration and sediment settling velocity in a tidal creek. *Continental Shelf Research*, *24*(15), 1659–1683. http://dx.doi.org/10.1016%2Fj.csr.2004.05.006

[36] Mikkelsen, O. A., Hill, P. S., Milligan, T. G., and Chant, R. J., 2005. In situ particle size distributions and volume concentrations from a LISST-100 laser particle sizer and a digital floc camera. *Continental Shelf Research*, *25*(16), 1959–1978. https://doi.org/10.1016/j.csr.2005.07.001

[37] Andrews, S., Nover, D., and Schladow, S. G., 2010. Using laser diffraction data to obtain accurate particle size distributions: the role of particle composition. *Limnology and Oceanography: Methods*, *8*(10), 507–526. https://doi.org/10.4319/lom.2010.8.507

[38] Graham, G. W., Davies, E. J., Nimmo-Smith, W. A. M., Bowers, D. G., and Braithwaite, K. M., 2012. Interpreting LISST-100X measurements of particles with complex shape using digital in-line holography. *Journal of Geophysical Research: Oceans*, *117*(C5). doi: 10.1029/2011JC007613

[39] Fettweis, M., and Baeye, M., 2015. Seasonal variation in concentration, size, and settling velocity of muddy marine flocs in the benthic boundary layer. *Journal of Geophysical Research: Oceans*, *120*(8), 5648–5667. https://doi.org/10.1002/2014JC010644

[40] Many, G., Bourrin, F., de Madron, X. D., Pairaud, I., Gangloff, A., Doxaran, D., Ody, A., Verney, R., Menniti, C., Berre, D. L., and Jacquet, M., 2016. Particle assemblage characterization in the Rhone River ROFI. *Journal of Marine Systems*, *157*, 39–51. http://dx.doi.org/10.1016/j.jmarsys.2015.12.010

[41] Pinet, S., Martinez, J. M., Ouillon, S., Lartiges, B., and Villar, R. E., 2017. Variability of apparent and inherent optical properties of sediment-laden waters in large river basins–lessons from in situ measurements and bio-optical modeling. *Optics express*, *25*(8), A283–A310. doi: 10.1364/OE.25.00A283

[42] Bader, H., 1970. The hyperbolic distribution of particle sizes. *Journal of Geophysical Research*, *75*(15), 2822–2830. doi: 10.1029/JC075i015p02822

[43] Jackson, G. A., Maffione, R., Costello, D. K., Alldredge, A. L., Logan, B. E., and Dam, H. G., 1997. Particle size spectra between 1 μm and 1 cm at Monterey Bay determined using multiple instruments. *Deep Sea Research Part I: Oceanographic Research Papers*, *44*(11), 1739–1767. doi: 10.1016/S0967-0637(97)00029-0

[44] Boss, E., Twardowski, M. S., and Herring, S., 2001. Shape of the particulate beam attenuation spectrum and its inversion to obtain the shape of the particulate size distribution. *Applied Optics*, *40*(27), 4885–4893. doi: 10.1364/AO.40.004885

[45] Woźniak, S. B., and Stramski, D., 2004. Modeling the optical properties of mineral particles suspended in seawater and their influence on ocean reflectance and chlorophyll estimation from remote

sensing algorithms. *Applied Optics*, *43*(17), 3489–3503. https://doi.org/10.1364/AO.43.003489

[46] Loisel, H., Nicolas, J. M., Sciandra, A., Stramski, D., and Poteau, A., 2006. Spectral dependency of optical backscattering by marine particles from satellite remote sensing of the global ocean. *Journal of Geophysical Research: Oceans*, *111*(C9). doi: 10.1029/2005JC003367

[47] Jonasz, M., 1983. Particle-size distributions in the Baltic. *Tellus B: Chemical and Physical Meteorology*, *35*(5), 346–358. https://doi.org/10.3402/tellusb.v35i5.14624

[48] Lee, B. J., Fettweis, M., Toorman, E., and Molz, F. J., 2012. Multimodality of a particle size distribution of cohesive suspended particulate matters in a coastal zone. *Journal of Geophysical Research: Oceans*, *117*(C3). doi: 10.1029/2011JC007552

[49] Hill, P. S., Syvitski, J. P., Cowan, E. A., and Powell, R. D., 1998. In situ observations of floc settling velocities in Glacier Bay, Alaska. *Marine Geology*, *145*(1–2), 85–94. https://doi.org/10.1016/S0025-3227(97)00109-6

[50] Fugate, D. C., and Friedrichs, C. T., 2003. Controls on suspended aggregate size in partially mixed estuaries. *Estuarine, Coastal and Shelf Science*, *58*(2), 389–404. http://dx.doi.org/10.1016/S0272-7714(03)00107-0

[51] Traykovski, P., Geyer, R., and Sommerfield, C., 2004. Rapid sediment deposition and fine-scale strata formation in the Hudson estuary. *Journal of Geophysical Research: Earth Surface*, *109*(F2). doi: 10.1029/2003JF000096

[52] Uncles, R. J., Stephens, J. A., and Law, D. J., 2006. Turbidity maximum in the macrotidal, highly turbid Humber Estuary, UK: Flocs, fluid mud, stationary suspensions and tidal bores. *Estuarine, Coastal and Shelf Science*, *67*(1–2), 30–52. https://doi.org/10.1016/j.ecss.2005.10.013

[53] Guo, C., He, Q., Guo, L., and Winterwerp, J. C., 2017. A study of in-situ sediment flocculation in the turbidity maxima of the Yangtze Estuary. *Estuarine, Coastal and Shelf Science*, *191*, 1–9. https://doi.org/10.1016/j.ecss.2017.04.001

[54] Wolanski, E., Huan, N. N., Nhan, N. H., and Thuy, N. N., 1996. Fine-sediment dynamics in the Mekong River estuary, Vietnam. *Estuarine, Coastal and Shelf Science*, *43*(5), 565–582. https://doi.org/10.1006/ecss.1996.0088

[55] Eisma, D., and Li, A., 1993. Changes in suspended-matter floc size during the tidal cycle in the Dollard estuary. *Netherlands Journal of Sea Research*, *31*(2), 107–117. doi: 10.1016/0077-7579%2893%2990001-9

[56] Mietta, F., Chassagne, C., Manning, A. J., and Winterwerp, J. C., 2009. Influence of shear rate, organic matter content, pH and salinity on mud flocculation. *Ocean Dynamics*, *59*(5), 751–763. http://dx.doi.org/10.1007/s10236-009-0231-4